MicroRNA-411 and its 5 '-IsomiR have distinct targets and functions and are differentially regulated in the vasculature under ischemia

Kwast, R.V.C.T. van der; Woudenberg, T.; Quax, P.H.A.; Nossent, A.Y.

Molecular Therapy
Original Article

MicroRNA-411 and Its 5′-IsomiR Have Distinct Targets and Functions and Are Differentially Regulated in the Vasculature under Ischemia

Reginald V.C.T. van der Kwast,[1,2] Tamar Woudenberg,[1,2] Paul H.A. Quax,[1,2] and A. Yaël Nossent[1,2,3,4]

[1]Department of Surgery, Leiden University Medical Center, Leiden 2333ZA, the Netherlands; [2]Einthoven Laboratory for Experimental Vascular Medicine, Leiden University Medical Center, Leiden 2333ZA, the Netherlands; [3]Department of Laboratory Medicine, Medical University of Vienna, Vienna 1090, Austria; [4]Department of Internal Medicine II, Medical University of Vienna, Vienna 1090, Austria

MicroRNAs are posttranscriptional regulators of gene expression. As microRNAs can target many genes simultaneously, microRNAs can regulate complex multifactorial processes, including post-ischemic neovascularization, a major recovery pathway in cardiovascular disease. MicroRNAs select their target mRNAs via full complementary binding with their seed sequence, i.e., nucleotides 2–8 from the 5′ end of a microRNA. The exact sequence of a mature microRNA, and thus of its 5′ and 3′ ends, is determined by two sequential cleavage steps of microRNA precursors, Drosha/DGCR8 and Dicer. When these cleavage steps result in nucleotide switches at the 5′ end, forming a so-called 5′-isomiR, this results in a shift in the mature microRNA's seed sequence. The role of 5′-isomiRs in cardiovascular diseases is still unknown. Here, we characterize the expression and function of the 5′-isomiR of miR-411 (ISO-miR-411). ISO-miR-411 is abundantly expressed in human primary vascular cells. ISO-miR-411 has a different "targetome" from WT-miR-411, with only minor overlap. The ISO-miR-411/WT-miR-411 ratio is downregulated under acute ischemia, both in cells and a murine ischemia model, but is upregulated instead in chronically ischemic human blood vessels. ISO-miR-411 negatively influences vascular cell migration, whereas WT-miR-411 does not. Our data demonstrate that isomiR formation is a functional pathway that is actively regulated during ischemia.

INTRODUCTION

MicroRNAs are ~22-nt-long small noncoding RNAs that regulate a wide range of physiological and pathological processes, including processes controlling cardiovascular function.[1–4] MicroRNAs are able to inhibit translation of protein-coding transcripts (mRNAs). A single microRNA can target hundreds of mRNAs, often regulating an entire network or pathway simultaneously.[5] The microRNA's "seed" sequence, nucleotides 2–8 from the 5′ end of the microRNA, predominantly determines target site recognition.[6,7]

The 5′ and 3′ ends of a microRNA are determined during the maturation steps of the primary transcript of the microRNA gene, known as the pri-miRNA.[8,9] First, the pri-miRNA is cleaved in the nucleus by the Microprocessor complex composed of ribonuclease (RNase) III enzyme DROSHA and DGCR8 to generate a hairpin-shaped precursor miRNA (pre-miRNA).[10] The pre-miRNA is exported to the cytoplasm, where it is processed further by RNase III enzyme DICER into a microRNA duplex.[11] The separate strands of the duplex can be incorporated into the RNA-induced silencing complex (RISC) as functional mature microRNAs.[12]

Typically, microRNAs are annotated as a single defined sequence and are listed as such in the principle public microRNA database, miRBase.[13] However, deep-sequencing studies have revealed that, for many microRNAs, sequence variants with slightly different 5′ and/or 3′ ends, known as isomiRs, can be generated from a single pri-miRNA hairpin.[14] This type of 5′ and 3′ heterogeneity derives from variations in processing by the DROSHA and/or DICER enzymes.[15–17] These isomiRs have been shown to function like canonical microRNAs, since they associate actively both with the RISC and with translational machinery polysomes.[9,18–20] IsomiRs with 5′ end variations, or 5′-isomiRs, are expected to be functionally important, as they result in an altered seed sequence, i.e., nucleotides 2–8 from the 5′ end, compared to the canonical microRNA; they are, therefore, expected to display altered target site selection. IsomiRs can have tissue-specific expression, and their expression profiles alone allow for discrimination between cancer types.[20–22] These observations suggest that isomiRs—5′-isomiRs in particular—can play an independent role in regulating pathophysiological processes. However, the specific roles of individual isomiRs and when they are regulated remain largely unknown.

MicroRNAs play a key role in cardiovascular disease.[3,4,23] Although cardiovascular diseases have a complex, multifactorial pathology, ischemia plays an intricate part in both the development and manifestation of most cardiovascular diseases. In response to ischemia, the

Received 12 June 2019; accepted 2 October 2019;
https://doi.org/10.1016/j.ymthe.2019.10.002.

Correspondence: A. Yaël Nossent, Department of Surgery, D6-28, Leiden University Medical Center, Albinusdreef 2, 2333ZA Leiden, the Netherlands.
E-mail: a.y.nossent@lumc.nl

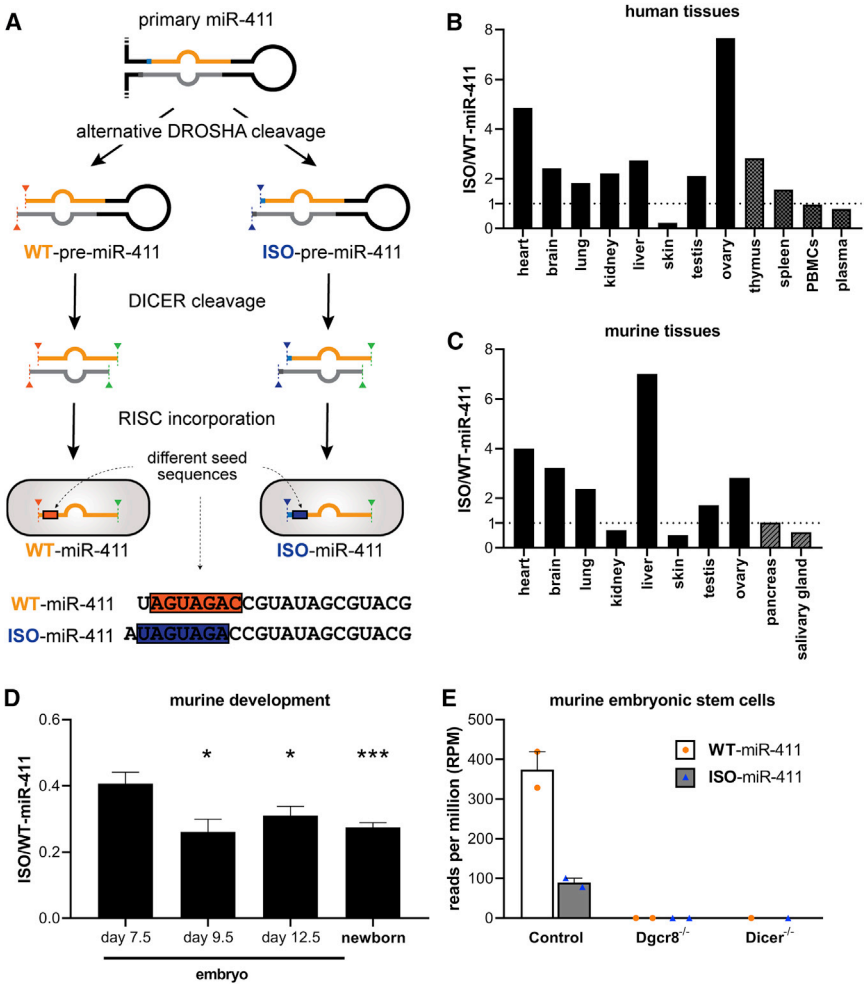

Figure 1. Biogenesis and Expression of miR-411 and its 5′-IsomiR

(A) The biogenesis of canonical WT-miR-411 and its 5′-isomiR (ISO-miR-411). Endonuclease DROSHA can cleave the primary miR-411 transcript at 2 distinct locations, which results in 2 different precursor microRNAs: WT-pre-miR-411 and ISO-pre-miR-411. Mature WT-miR-411 and ISO-miR-411 are produced after their respective pre-miRNAs and preferential incorporation into the RISC. Compared to WT-miR-411, ISO-miR-411 has an additional nucleotide at its 5′ end (in blue) and, therefore, has a different seed sequence. (B–D) Public miRNA-seq datasets were analyzed to examine the prevalence of ISO-miR-411 relative to WT-miR-411 in human tissues (B; n = 1), in murine tissues (C; n = 1), and during murine development (D; n ≥ 4). (E) Expression of WT-miR-411 and ISO-miR-411 in public miRNA-seq data from control murine embryonic stem cells and murine embryonic stem cells with a knockout of either *Dgcr8* (*Dgcr8*$^{-/-}$) or *Dicer* (*Dicer*$^{-/-}$) (n = 1 or 2). In (D) and (E), data are presented as mean ± SEM. *p < 0.05; and ***p < 0.001 versus embryos of day 7.5 by two-sided Student t test.

adaptive growth of blood vessels, known as neovascularization, helps to restore blood flow. We have shown that the microRNAs from a large microRNA gene cluster located on the long arm of human chromosome 14 (14q32) are regulated during ischemia in mice and can directly affect neovascularization.[24] Interestingly, recent studies have shown that one of these 14q32 microRNAs, miR-411, has a 5′-isomiR.[25] This miR-411 5′-isomiR (ISO-miR-411) has an additional 5′ adenosine compared to the canonical wild-type miR-411 (WT-miR-411). The isomiR appears to be the result of a single nucleotide shift in DROSHA's cleavage of the primary miR-411 transcript (pri-miR-411) (Figure 1A). Currently, however, the prevalence, regulation, and function of ISO-miR-411 are unknown.

In this study, we demonstrate that ISO-miR-411 is at least 5-fold more abundant than WT-miR-411 in primary human vascular cells and in venous tissue samples from patients with peripheral artery disease (PAD). Additionally, we show that ISO-miR-411 and WT-miR-411 expression is differentially regulated in cultured vascular fibroblasts under ischemic conditions, and we confirm these findings in a murine hindlimb ischemia (HLI) model. Finally, we demonstrate that ISO-miR-411, indeed, targets a different and larger set of genes than WT-miR-411, resulting in functional differences in angiogenesis *in vitro*.

RESULTS

Prevalence of ISO-miR-411

We analyzed public microRNA sequencing (miRNA-seq) datasets to examine the prevalence of ISO-miR-411 relative to WT-miR-411 in human and murine tissues. The miRNA-seq data showed that ISO-miR-411 is expressed in all examined tissues. ISO-miR-411 expression relative to WT-miR-411 expression varied strongly per tissue (Figures 1B and 1C). For example, in both human and murine datasets, the ratio of ISO-miR-411 to WT-miR-411 (ISO/WT-miR-411) was below 0.5 in skin tissue, while the ratio was approximately 4 in cardiac tissue. Furthermore, ISO/WT-miR-411 is decreased in datasets from murine whole-body tissue of 9.5-day-old embryos, 12.5-day-old embryos, and newborn mice when compared to 7.5-day-old embryos (ISO/WT-miR-411: 0.26 ± 0.04, 0.31 ± 0.03, and 0.27 ± 0.01 versus 0.41 ± 0.03; $p < 0.03$, $p < 0.05$, and $p < 0.001$, respectively) (Figure 1D). These observations suggest that WT-miR-411 and ISO-miR-411 expressions are differentially regulated over time. Both WT-miR-411 and ISO-miR-411 were confirmed to be products of the microRNA maturation pathway, since both their expressions are abolished in murine embryonic stem cells deficient for either Dgcr8 or Dicer (Figure 1E).

WT-miR-411 and ISO-miR-411 Expression in Vascular Cells

We then determined whether ISO-miR-411 is also abundantly expressed in primary human umbilical arterial fibroblasts (HUAFs)

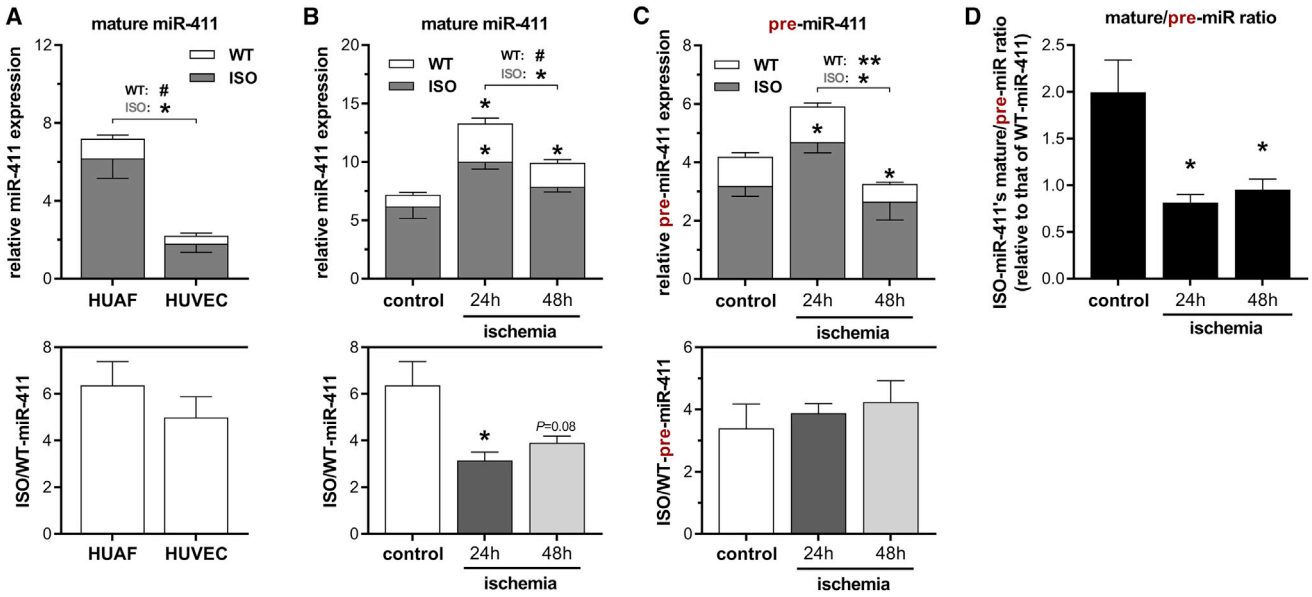

Figure 2. WT-miR-411 and ISO-miR-411 Expression in Primary Vascular Cells under Ischemic Conditions

(A–C) 5′DB-PCR was used to quantify WT-miR-411 (white) and ISO-miR-411 (dark gray) transcripts. In each graph, relative expression is presented in the upper panel, while the corresponding ISO/WT-miR-411 ratio is shown in the bottom panel. (A) WT-miR-411 and ISO-miR-411 expression in HUVECs and HUAFs. (B and C) Regulation of mature miR-411 expression (B) and pre-miR-411 expression (C) and their respective ISO/WT ratios after subjecting HUAFs to ischemic conditions for 24 h or 48 h. Ischemic conditions were induced by a combination of hypoxia and serum starvation, resulting in hypoxia signaling and cell-cycle arrest (Figure S2). miR-411 expression was normalized to U6 and presented as fold of WT-miR-411 expression in the HUAF control group. (D) The mature/pre-miR ratio of ISO-miR-411 relative to the WT-miR-411's mature/pre-miR ratio as calculated from data in (B) and (C). All data are shown as mean ± SEM (n = 3). #$p < 0.1$; *$p < 0.05$; and **$p < 0.01$ versus control condition unless otherwise indicated by two-sided Student t test.

and human umbilical venous endothelial cells (HUVECs). Expression of WT-miR-411 and ISO-miR-411 were quantified using 5′ Dumbbell-PCR (5′DB-PCR), specifically designed and validated to distinguish between the highly similar sequences of WT-mir-411 and ISO-miR-411 (Figure S1). We found that ISO-miR-411 is expressed at least 5-fold higher than WT-miR-411 in both cell types (Figure 2A). However, the expression of both WT-mir-411 and ISO-miR-411 was approximately 3-fold higher in HUAFs compared to HUVECs (Figure 2A, $p = 0.02$ and $p = 0.07$, respectively). Therefore, subsequent experiments were performed in HUAFs.

We then cultured HUAFs under ischemic conditions to examine whether miR-411 expression is regulated under ischemia. Both 24 h and 48 h of ischemic culture conditions successfully induced hypoxic signaling and cell-cycle arrest, as demonstrated by increased expression of *HIF1A*, *VEGFA*, and *SDF1*, and *p53*, respectively (Figure S2). After 24 h of ischemia, WT-miR-411 expression increased by 3.3-fold, while ISO-miR-411 expression increased by only 1.6-fold (Figure 2B, upper panel, $p = 0.01$ and $p = 0.03$ versus control, respectively), decreasing ISO/WT-miR-411 from 6.4 ± 1.0 under control conditions to 3.2 ± 0.4 after 24 h of ischemia (Figure 2B, lower panel, $p = 0.04$). After 48 h of ischemic conditions, both WT-miR-411 and ISO-miR-411 expression decreased again (Figure 2B, upper panel, $p = 0.08$ and $p < 0.05$ versus 24 h, respectively), but ISO/WT-miR-411 remained decreased (Figure 2B, lower panel, 48-h ratio: 3.9 ± 0.3, $p = 0.08$). These data demonstrate that mature WT-miR-411 and ISO-miR-411 are differentially regulated under ischemia in human primary vascular fibroblasts.

WT-pre-miR-411 and ISO-pre-miR-411 Expression

To determine at which step in microRNA processing WT-miR-411 and ISO-miR-411 are regulated, we also quantified wild-type pre-miR-411 (WT-pre-miR-411) and isomiR pre-miR-411 (ISO-pre-miR-411) expression using 5′DB-PCR. Similar to mature miRNA levels, ISO-pre-miR-411 expression was higher than WT-pre-miR-411 expression in primary arterial fibroblasts and followed a similar pattern under ischemic conditions: increased expression after 24 h of ischemia and subsequently decreased expression after 48 h of ischemia (Figure 2C, upper panel). However, ISO/WT-pre-miR-411 did not decrease under ischemia and even appeared to increase slightly, although not statistically significantly (Figure 2C, lower panel). To examine whether ISO-miR-411's mature and pre-miR levels are inversely correlated, we calculated the ISO-miR-411's mature/pre-miR ratio relative to the WT-miR-411's mature/pre-miR ratio. The ratio is significantly decreased in fibroblasts grown under ischemia (Figure 2D). These results suggest that, while Drosha cleavage introduces differential expression between WT-pre-miR-411 and ISO-pre-miR-411, it is the final maturation step that induces differential expression of mature WT-miR-411 and ISO-miR-411 under ischemia.

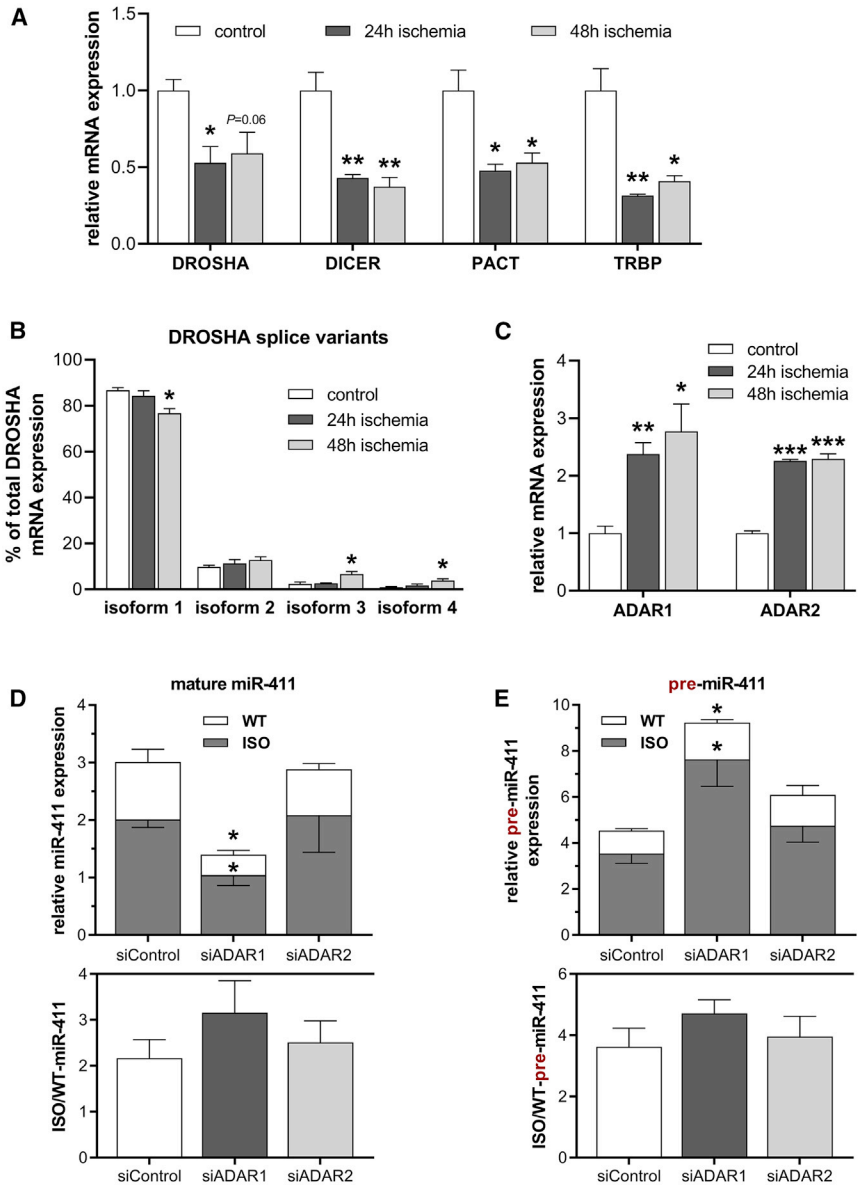

Figure 3. Expression of miRNA Biogenesis Factors and the Role of ADARs in miR-411 Biogenesis

(A) Expression of factors involved in miRNA biogenesis after culturing HUAFs under control or ischemic conditions, as quantified by qRT-PCR. (B) Relative expression of individual *DROSHA* isoforms as percentage of total *DROSHA* mRNA expression. (C) Expression of *ADAR1* and *ADAR2* in control or ischemic HUAFs quantified by qRT-PCR. In (A)–(C): *p < 0.05; **p < 0.01; and ***p < 0.001 versus control condition by two-sided Student t test. (D and E) ADAR1 and ADAR2 were knocked down in HUAFs through transfection of an *ADAR1*-targeting or *ADAR2*-targeting siRNA (siADAR1 and siADAR2, respectively). The subsequent effects on WT- and ISO-miR-411 expression (D) and on WT- and ISO-pre-miR-411 expression (E) were determined as in Figure 2 and compared to transfection with a negative-control siRNA (siNegCtrl). In (D) and (E), *p < 0.05 versus siNegCtrl by two-sided Student t test. All data are presented as mean ± SEM (n = 3).

Regulation of Factors Involved in miRNA Biogenesis

In agreement with previous studies, we observed downregulation of important components of the microRNA machinery under ischemic conditions, including *DROSHA* and *DICER* (Figure 3A).[26,27] *DROSHA* has several isoforms, 2 of which were upregulated under ischemia but still expressed at relatively low levels (Figure 3B). The dominant isoform, on the other hand, was modestly downregulated. Differential regulation of *DROSHA* isoforms is, therefore, unlikely to explain differential regulation of WT-miR-411 versus ISO-miR-411. The enzymes adenosine deaminase acting on RNA 1 (*ADAR1*) and *ADAR2*, however, were upregulated under ischemia (Figure 3C), as was shown previously.[28,29] Although they were initially described to regulate RNA editing, both ADAR1 and ADAR2 have been shown to regulate microRNA processing.[29–31] Indeed, when we specifically inhibited ADAR1 using small interfering RNAs (siRNAs) (Figure S3), both WT-miR-411 and ISO-miR-411 are downregulated (Figure 3D). Notably, both pre-miRNAs are upregulated, indicating that ADAR1 facilitates processing of both WT- and ISO-pre-miR-411 (Figure 3E). ADAR1 knockdown did not affect ISO/WT-miR-411, indicating that ADAR1 does not selectively bind either isoform of miR-411.

WT-miR-411 and ISO-miR-411 Expression *In Vivo*

Next, we examined WT-miR-411 and ISO-miR-411 expression in distinct whole-muscle tissues (adductor, gastrocnemius, and soleus) of C57BL/6 mice before and after induction of acute HLI. We observed differences in baseline miR-411 expression between the different muscles (Figure 4A). Consistent with our *in vitro* results, expression of both WT-miR-411 and ISO-miR-411 transiently increased in the ischemic gastrocnemius and soleus muscles 1 day (T1) after HLI compared to before surgery (T0). Also consistent with the *in vitro* data, ISO-miR-411/WT-miR-411 decreased at both T1 and T3. The decrease in the ISO/WT ratio was not observed at the pre-miR-411 stage in either ischemic muscles, which is also consistent with our *in vitro* results (Figure 4B). Furthermore, the ISO-miR-411's relative mature/pre-miR ratio was decreased at T3 in the ischemic gastrocnemius and soleus muscles, suggesting that ISO-pre-miR-411 processing is also lowered after acute ischemia *in vivo* compared to processing of WT-pre-miR (Figure 4C). In this particular mouse model, the adductor remains relatively normoxic.[32] Accordingly, we did not observe changes in

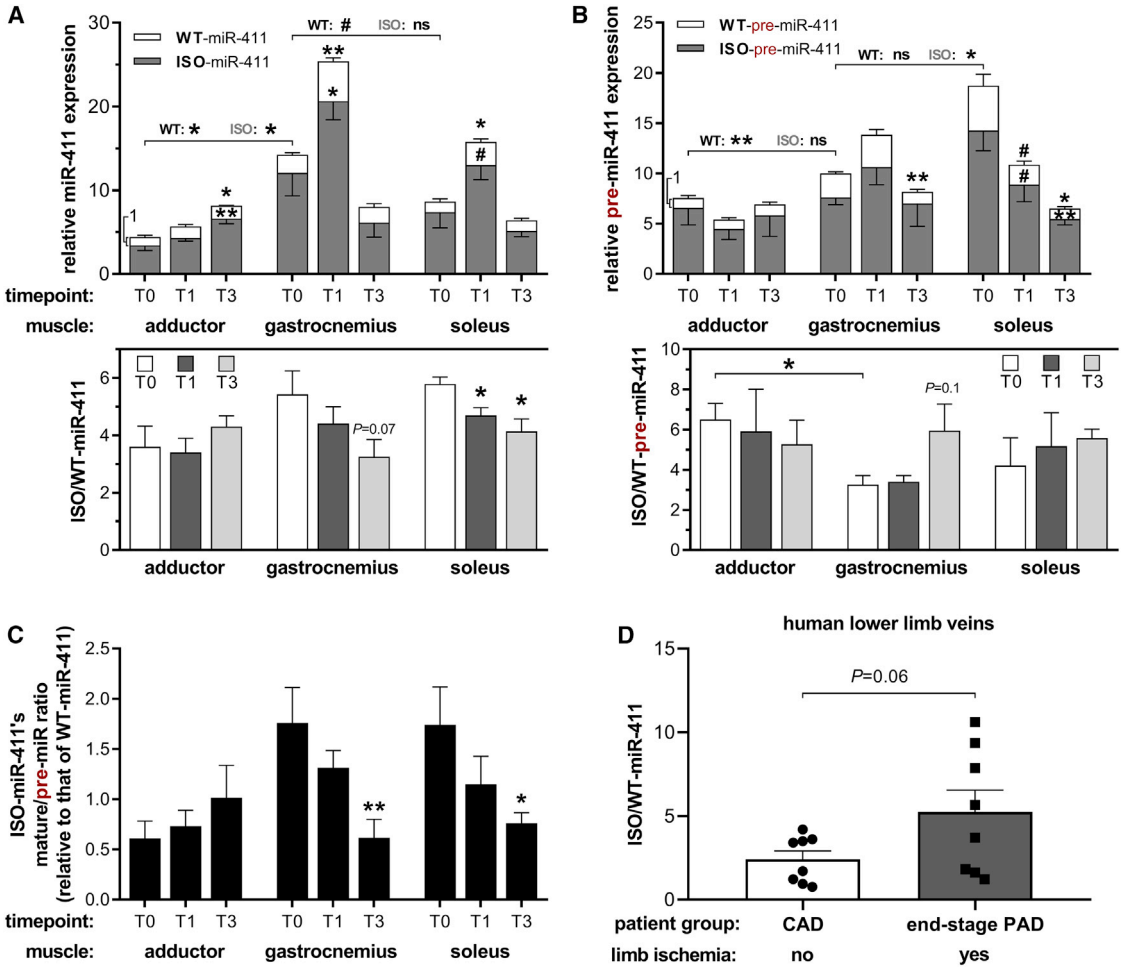

Figure 4. miR-411 Regulation after Acute Hindlimb Ischemia in Mice and in Human Chronically Ischemic Lower Limb Veins

(A–C) miR-411 expression was measured by 5′DB-PCR in three different mouse muscle tissues were harvested before (T0) or 1 and 3 days after induction of hindlimb ischemia (T1 and T3, respectively) (n = 4 per group). While the gastrocnemius and soleus experience ischemia after surgery, the adductor remains relatively normoxic due to its more upstream anatomical location.[32] Regulation of mature miR-411 expression (A) and pre-miR-411 expression (B) and ISO-miR-411's relative mature/pre-miR ratio (C) after hindlimb ischemia are indicated as described in Figure 2. (D) ISO/WT-miR-411 ratio in LLV samples from normoxic LLV samples (n = 8) from patients with CAD compared to critically ischemic LLV samples (n = 8) from patients with end-stage PAD, undergoing lower limb amputation. All data are presented as mean ± SEM. #p < 0.1; *p < 0.05; **p < 0.01; and ***p < 0.001 versus T0 unless otherwise indicated by two-sided Student t test. Each symbol is associated with the bar directly underneath it.

ISO-mir-411/WT-miR-411 (Figures 4A–4C). These results demonstrate that WT-miR-411 expression and ISO-miR-411 expression are also differentially regulated in response to ischemia *in vivo*.

WT-miR-411 and ISO-miR-411 Expression in Patients

To examine miR-411 expression in patients with chronic ischemia, we measured the ISO-miR-411/WT-miR-411 ratio in chronically ischemic lower leg vein (LLV) samples from patients with end-stage PAD, undergoing lower limb amputation. We compared these to asymptomatic LLV samples from patients with coronary artery disease (CAD) undergoing coronary artery bypass surgery. We found that ISO-miR-411 was more abundantly expressed than WT-miR-411 in all LLV samples. Furthermore, ISO/WT-miR-411 was 2.2-fold higher in the chronically ischemic LLV samples compared to the normoxic LLV samples (p = 0.06) (Figure 4D). These data show that WT-miR-411 and ISO-miR-411 are also differentially expressed during chronic ischemia in humans; however, expression patterns clearly differ from those under acute ischemia.

In Silico Targetome Predictions

The ISO-miR-411 has a seed sequence that is different from any other human microRNA seed-sequence (http://www.targetscan.org, release 7.2)[33] and will, therefore, have a unique targetome. To examine the differences between the targetomes of WT-miR-411 and ISO-miR-411, we used three distinct target prediction algorithms. We found that the targetome of ISO-miR-411 contains approximately twice as many putative

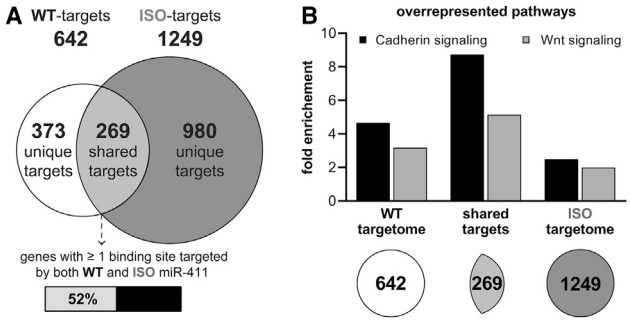

Figure 5. *In Silico* Prediction of WT-miR-411 and ISO-miR-411 Targetomes
(A) Venn diagram of putative targetomes for WT-miR-411 (white) and ISO-miR-411 (dark gray) representing the putative target genes that were unanimously identified by all three prediction algorithms used. (B) Significantly enriched pathways within the different targetomes and within the subset of shared targets (details are given in Table S1).

target genes than the WT-miR-411 targetome (Figure 5A). The majority of putative target genes are unique to either the WT- or the ISO-miR-411 targetome (58% and 78%, respectively). In fact, approximately half of the overlapping targets (129 of 269, 48%) are shared targets only because the mRNAs have independent binding sites for both WT-miR-411 and ISO-miR-411, rather than containing a single binding site that can be targeted by both WT-miR-411 and ISO-miR-411.

Pathway enrichment analyses of the targetomes using the PANTHER algorithm[34] revealed that both the WT-miR-411 and ISO-miR-411 targetomes contain overrepresentation of genes related to Cadherin signaling and Wnt signaling, most of which are shared targets (Figure 5B; Table S1).

Validation of Differential Target Regulation

In order to validate whether there are, indeed, WT-miR-411-specific targets, ISO-miR-411-specific targets, and shared targets, we selected at least one gene from each target group that could be linked to the response to ischemia: transforming growth factor beta-2 (*TGFB2*; target of WT-miR-411), cadherin-2 (*CDH2*, shared target), cadherin-6 (*CDH6*, shared target), tissue factor (*F3*, target of ISO-miR-411), and angiopoietin-1 (*ANGPT1*, target of ISO-miR-411). MicroRNA binding to these genes was examined by incorporating their endogenous 3′UTR putative binding sequences in luciferase reporter constructs and performing reporter gene assays (Figure 6A). Luciferase activity of the WT-miR-411 binding-site-containing *TGFB2* sequence was, indeed, only repressed by WT-miR-411 to 89% ± 1% ($p = 0.01$) and not by ISO-miR-411 ($p = 0.5$). Luciferase activity of sequences from shared targets *CDH2* and *CDH6* was reduced by both WT-miR-411 and ISO-miR-411. Finally, luciferase activity of ISO-miR-411 binding-site-containing *F3* and *ANGPT1* sequences was repressed only by ISO-miR-411 to 85% ± 2% ($p = 0.01$) and 56% ± 5% ($p = 0.01$), respectively.

Next, we overexpressed either WT-miR-411 or ISO-miR-411 in HUAFs and examined endogenous target mRNA regulation (Figure 6B). Consistent with luciferase results, treatment with WT-miR-411 decreased endogenous expression of *TGFB2*, *CDH2*, and, to a lesser extent, *CDH6* by 43% ± 9% ($p = 0.04$), 28% ± 5% ($p = 0.03$), and 23% ± 20% ($p = 0.3$), respectively, but did not decrease *F3* or *ANGPT1* expression ($p = 0.5$, and $p = 0.7$). Conversely, treatment with ISO-miR-411 did not affect *TGFB2* expression ($p = 0.7$), while expression of *CDH2*, *CDH6*, *F3*, and *ANGPT1* was repressed by 40% ± 5% ($p = 0.01$), 30% ± 10% ($p = 0.1$), 28% ± 6% ($p = 0.04$), and 36% ± 7% ($p = 0.03$), respectively.

To confirm whether endogenous target mRNA regulation, indeed, results in regulation of protein levels, we selected TGFB2 as the target for the WT-miR-411 and ANGPT1 as the target for ISO-miR-411. No secretion of TGFB2 protein could be detected in the conditioned medium of our HUAFs (data not shown), but TGFB2 was detected in whole-cell lysates (Figure 6C). Consistent with our findings on mRNA levels, TGFB2 protein was significantly downregulated after treatment with WT-miR-411 ($p = 0.04$) but not after treatment with ISO-miR-411 ($p = 0.4$). ANGPT1 is secreted by HUAFs, and ANGPT1 levels in HUAF conditioned medium remained unaltered after treatment with WT-miR-411 ($p = 0.8$) but were decreased after treatment with ISO-miR-411 ($p = 0.005$) (Figure 6D). These results confirm that ISO-miR-411 has a unique targetome that only partially overlaps with the targetome of WT-miR-411.

Functional Effects of miRNA Editing

Functional effects of WT-miR-411 and ISO-miR-411 were examined by measuring HUAF cell migration using scratch-wound healing assays after overexpression of either microRNA. Changes in percentage of ISO/WT-miR-411 after microRNA overexpression were validated using 5′DB-PCR (Figure S4). Treatment with ISO-miR-411 reduced wound healing by 24% ± 3% ($p = 0.01$) compared to the control microRNA treatment, while WT-miR-411 treatment did not ($p = 0.3$) (Figure 7).

DISCUSSION

In this study, we found that the 5′-isomiR of miR-411, ISO-miR-411, is more abundant than miR-411 itself (WT-miR-411) in primary human vascular fibroblasts and in human venous tissue samples. We demonstrate that ISO-miR-411 expression and WT-miR-411 expression are differentially regulated in response to ischemia *in vitro* as well as *in vivo* in a murine HLI model. We show that the observed differential expression is regulated during processing from pre-miR-411 to mature miRNA, rather than during the biogenesis of the WT-pre-miR-411 and ISO-pre-miR-411. The seed sequence of ISO-miR-411 is shifted by 1 nucleotide, compared to WT-miR-411. We demonstrate that this seed-sequence shift causes ISO-miR-411 to target a unique and larger set of mRNAs compared to WT-miR-411, leading to functional changes in the cellular response to ischemia.

We found that the expression of ISO-miR-411, compared to that of WT-miR-411, varies between tissues and that ISO-miR-411 expression is at least 3-fold higher than that of WT-miR-411 in human vascular cells and whole vascular tissue. These findings are consistent

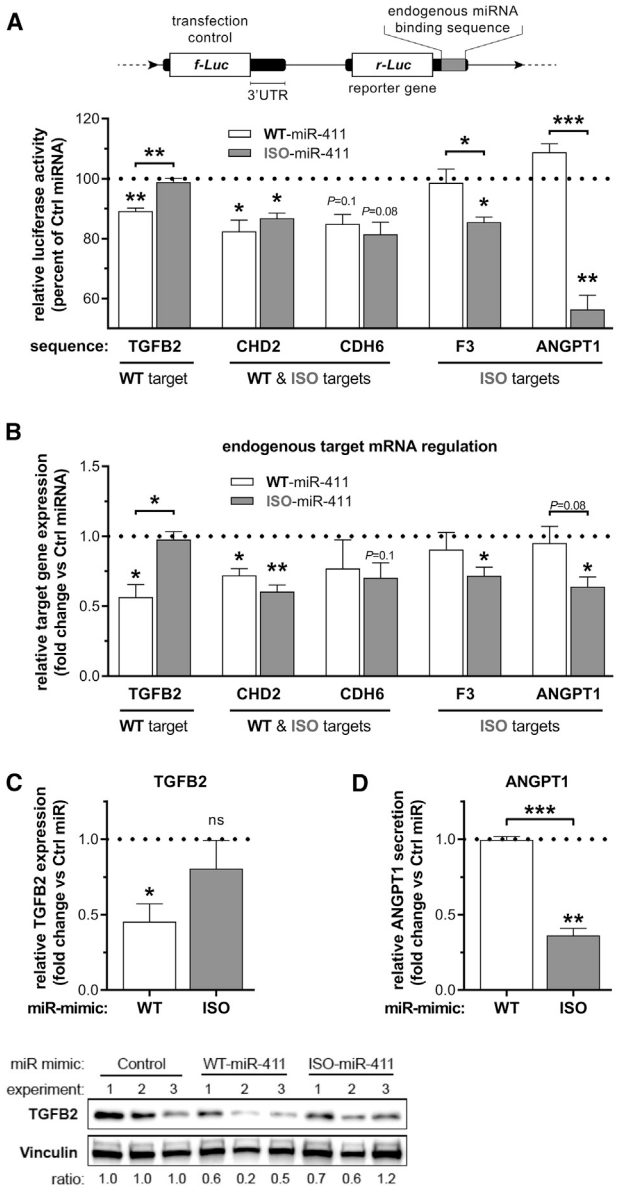

Figure 6. Validation of Differential Target Sequence Binding and Endogenous Target Regulation

(A) Schematic representation of the luciferase constructs that were used to examine the binding of WT-miR-411 and ISO-miR-411 to endogenous miRNA binding sequences from selected putative target genes. The selected genes predicted targets of either WT-miR-411 or ISO-miR-411, or both, as indicated. Constructs were co-transfected with WT-miR-411, ISO-miR-411, or a non-targeting miRNA mimic (Ctrl miRNA) into HeLa cells. MicroRNA-specific target site binding was assessed by examining luciferase reporter activity relative to that of the Ctrl miRNA (dotted line). (B) Endogenous target mRNA regulation relative to Ctrl miRNA treatment after transfection of HUAFs with microRNA mimics as indicated. (C) Relative TGFB2 protein expression in HUAF whole-cell lysates after transfection with indicated miRNA mimics as determined by western blot. Expression was normalized per independent experiment to stable household protein vinculin and expressed relative to Ctrl miRNA. (D) Relative ANGPT1 levels in the conditioned medium of transfected HUAFs. All data points represent normalized averages obtained from 3 independent experiments and are presented as mean ± SEM. *$p < 0.05$; **$p < 0.01$; and ***$p < 0.001$ by one-sample t test versus Ctrl miRNA or two-sided Student t test to compare WT-miRNA versus ISO-miRNA treatments.

with those of previous studies that have shown that isomiRs, in general, can have tissue-specific expression.[20–22] The majority of these tissue-specific isomiRs were 3′-isomiRs, however, which have an unaltered seed sequence. Nevertheless, a recent study showed that expression of a subset of 5′-isomiRs was tumor specific enough to allow for tumor classification. Despite these findings, it remained unclear whether changes in the ISO/WT-miRNA ratio can be induced in response to pathophysiological changes. With the differential regulation of WT-miR-411 and ISO-miR-411 expression under ischemia, we provide evidence that 5′-isomiR expression can, indeed, respond to pathophysiological changes.

5′-isomiRs are generally formed by cleavage variations of either DROSHA or DICER during miRNA biogenesis.[9,35] miR-411 is located on the 5′-pri-miRNA arm, which means that DROSHA cleavage introduces the 5′ end variation when cutting pri-miR-411 to pre-miR-411. We found abundant ISO-pre-miR-411 expression, which confirms that alternative DROSHA cleavage is responsible for the 5′ end variation of miR-411. The factors that influence alternative DROSHA cleavage are largely unknown. We hypothesized that DROSHA's different isoforms could be responsible for cleavage variation. However, isoform expression profiles suggested that this is unlikely, since the transcript of one isoform clearly dominates total *DROSHA* expression in our primary human fibroblasts.

It is assumed that the rate of differential cleavage that introduces the 5′ end variation determines the isomiR's abundance.[36,37] We found that ISO/WT-pre-miR-411 increased under acute ischemia, while the mature ISO/WT-miR-411 decreased significantly. These findings demonstrate that the differential regulation of WT-miR-411 and ISO-miR-411 under ischemia is not caused by changes in DROSHA cleavage. If not by DROSHA, changes in ISO/WT-miR-411 can be caused either by changes in DICER substrate selection and cleavage or by altered microRNA turnover rates. Indeed, it has been shown that isomiRs of the same microRNA display different turnover rates. Although still poorly understood, a larger body of evidence indicates sequence variations in the 3′ end of the microRNA as responsible for altered turnover rates.[38] However, Guo et al.[39] showed for miR92b-3p, also a vasoactive microRNA, that isoforms with an adenosine added in front of the original uracil at the 5′ end, similar to ISO-miR-411, are less stable and cleared faster. This was found in unchallenged HDMYZ cells however, so it was not investigated whether ischemia would alter these clearance rates. Although we cannot exclude an effect of altered isomiR turnover under ischemia, we do provide evidence here that the altered ISO/WT-miR-411 is, at least in part, introduced during the final maturation step from pre-miR-411 to mature miR-411.

Several studies have shown that the ISO/WT-miRNA ratios of 5′-isomiRs generated by alternative DICER cleavage can be

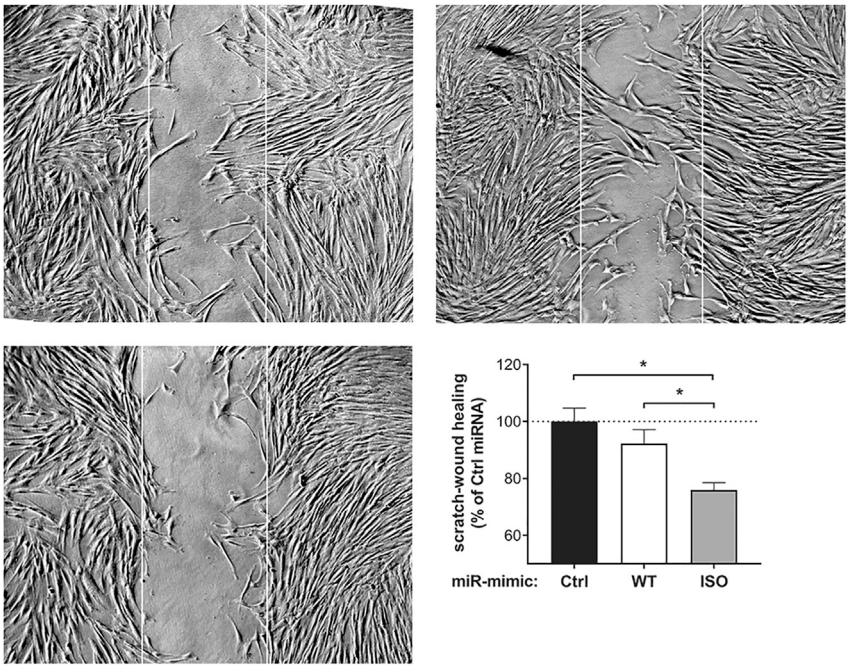

Figure 7. The Effect of WT-miR-411 and ISO-miR-411 on *In Vitro* Scratch-Wound Healing

Representative images and quantification of HUAF scratch-wound healing after transfection with either WT-miR-411 (WT), ISO-miR-411 (ISO), or non-targeting miRNA mimic (Ctrl). White lines indicate original scratch wound area. Data points represent averages obtained from 3 independent experiments and are presented as mean ± SEM. *$p < 0.05$ by two-sided Student t test.

modulated by DICER cofactors TRBP and PACT.[36,40] While we did observed a decrease in the expression of *TRBP* and *PACT* under ischemia, this is unlikely to be responsible for regulating ISO/WT-miR-411, since the DICER cleavage site is identical for both miR-411 variants. However, we observed an initial increase of miR-411 expression under ischemia, which coincided with increased *ADAR1* and *ADAR2* expression. ADAR1 facilitates microRNA biogenesis via direct interaction with DICER in order to increase its cleavage efficiency.[30,41,42] Therefore, we hypothesized that ADARs play a role in regulation of WT-miR-411 and ISO-miR-411. Even though ADARs did not affect ISO/WT-miR-411, we found that knockdown of ADAR1 decreased WT- and ISO-miR-411 expression. Simultaneously, expression of their pre-miRNAs increased, indicating that pre-miR-411 processing efficiency was decreased. These findings add to the growing body of evidence that ADAR1 regulates microRNA expression and function under pathological conditions.[29,31,42,43] Besides ADAR1, many other RNA-binding proteins (RBPs) can impact the processing of microRNAs in a highly (sequence-)specific manner.[44] We have recently shown that the Cold Inducible RBP (CIRBP) and HADHB regulate processing of miR-329 and miR-495 but not of other closely related microRNAs under ischemia.[45] The myocyte enhancer factor 2A (MEF2A), which is known as a DNA-binding protein, also functions as an RBP, regulating microRNA biogenesis in a microRNA-specific manner.[46] A recent study by Treiber et al.[47] even showed that many, if not all, individual microRNAs have their own RBP to facilitate microRNA biogenesis. Therefore, it is not at all unlikely that that there are also isomiR-specific RBPs that regulate their processing and expression.

We found that the ISO/WT-miR-411 ratio is decreased in response to acute ischemia, in cultured fibroblasts, but also in murine muscle tissue. ISO-miR-411 has a unique seed sequence that is different from that of WT-miR-411 as well as from that of any other any known microRNA.[33] We demonstrate that WT-miR-411, but not ISO-miR-411, downregulates expression of TGFB2, a cytokine that affects many cellular processes, including angiogenesis.[48,49] ISO-miR-411 on the other hand, specifically downregulates the expression of both F3 and ANGPT1, which can both stimulate cell migration and wound healing.[50–53] Consistent with these findings, our *in vitro* scratch-wound healing assays demonstrate that ISO-miR-411 treatment decreases cell migration and wound closure, whereas WT-miR-411 does not. These findings imply that ISO-miR-411 is downregulated in response to acute ischemia in order to allow for a pro-angiogenic response that is further facilitated by an increase in the pro-angiogenic WT-miR-411. In patients with end-stage PAD, the pro-angiogenic response is generally insufficient. We observed an increase in the ISO-miR-411/WT-miR-411 ratio in lower limb veins (LLVs) from end-stage PAD patients, which may contribute to the lack of efficient neovascularization in these patients.

In conclusion, we demonstrate that miR-411 has a 5′-isomiR that is abundantly expressed in the vasculature. Maturation of WT-pre-miR-411 and that of ISO-pre-miR-411 are differentially regulated in the response to acute ischemia, resulting in a decreased mature ISO/WT-miR-411 ratio, both *in vitro* and *in vivo*. ISO-miR-411 has a unique targetome, which includes the pro-angiogenic genes *F3* and *ANGPT1*. In contrast to WT-miR-411, ISO-miR-411 decreased *in vitro* scratch-wound healing, demonstrating that ISO-miR-411 and WT-miR-411 have distinct biological functions.

By showing that the formation of isomiRs is an actively regulated process and that isomiRs have individual sets of target genes that differ from that of the canonical microRNAs, we demonstrate, for the first time in a cardiovascular setting, that yet another level of active regulation of gene and protein expression exists within the emerging field of noncoding RNAs. At this point, the impact of the reported findings cannot yet be overseen, but we are convinced that isomiRs will prove to be of importance in future microRNA-based therapeutic strategies.

MATERIALS AND METHODS

Identification of Vasoactive MicroRNAs Containing A-to-I Editable Adenosines

Publicly available miRNA-seq datasets were analyzed to examine ISO-miR-411 versus WT-miR-411 expression in human and murine tissues.

For human tissues, the following datasets were analyzed using the "miR-seq browser" function of the miRGator webtool (http://mirgator.kobic.re.kr):[54] SRX050631 (heart), GSM548639 (whole brain), SRX050632 (lung), SRX050637 (kidney), SRX050638 (liver), GSM769005 (skin), SRX050635 (testes), SRX050634 (ovary), SRX050633 (thymus), SRX050636 (spleen), GSM494810 (PBMCs), and GSM1279746 (plasma).

For murine tissues, the following datasets were analyzed using the IsomiR Bank webtool (https://mcg.ustc.edu.cn/bsc/isomir):[55] GSM539868 (heart), GSM539869 (brain), GSM539870 (lung), GSM539872 (kidney), GSM539871 (liver), GSM539874 (skin), GSM539877 (testes), GSM539878 (ovaries), GSM539873 (pancreas), GSM539876 (salivary glands), GSM510457–GSM510460 (day-12.5 embryos), GSM510461–GSM510464 (day-9.5 embryos), GSM510465–GSM510468 (day-7.5 embryos), GSM510445–GSM510456 (whole-body newborn mice), GSM314552 and GSM314558 (WT ESCs), GSM314557 and GSM314559 (DGCR8 knockout ESCs), and GSM314553 (Dicer knockout ESCs).

In each case, we extracted the number of WT-miR-411 and ISO-miR-411 reads or reads per million within a particular sample. The ISO/WT-miR-411 ratio was simply calculated by dividing the number of ISO-miR-411 reads by the number of WT-miR-411 reads.

Isolation of Primary Vascular Cells from Human Umbilical Cords

Isolation and culturing of primary HUAFs was performed as described previously.[24,29]

In brief, umbilical cords were collected anonymously from full-term pregnancies at the Leiden University Medical Center and used for either HUAF or HUVEC isolation. Collection and processing of umbillical cords were performed in complicance with local and national regulations.

For HUAF isolation, the tunica adventitia was removed from the umbilical artery and incubated overnight in serum-rich medium (DMEM GlutaMAX, Invitrogen-GIBCO, Auckland, New Zealand), 10% heat-inactivated fetal bovine serum (FBS; PAA Laboratories, Pasching, Austria), 10% heat-inactivated human serum, 100 U penicillin, and 100 μg/mL streptomycin (Lonza, Basel, Switzerland) and nonessential amino acids (GIBCO, #11140050). The next day, the adventitia was incubated in a 2 mg/mL collagenase type II solution (Worthington, Lakewood, NJ, USA) at 37°C. The resulting cell suspension was filtered over a 70-μm cell strainer, pelleted, resuspended, and plated in HUAF culture medium (DMEM GlutaMAX [Invitrogen], 10% heat-inactivated FBS [PAA], and 100 U penicillin and 100 μg/mL streptomycin [Lonza]).

HUVECs were isolated from the umbilical veins by infusing a flushed vein with 0.75 mg/mL collagenase type II (Worthington) and incubated at 37°C for 20 min. The cell suspension was collected, pelleted, and resuspended in HUVEC culture medium: M199 (PAA), 10% heat-inactivated human serum (PAA), 10% heat-inactivated newborn calf serum (PAA), 100 U penicillin and 100 μg/mL streptomycin (Lonza), 150 μg/mL endothelial cell growth factor (kindly provided by Dr. Koolwijk, VU Medical Center, Amsterdam, the Netherlands), and 5 U/mL heparin (LEO Pharma, Ballerup, Denmark). HUVECs were cultured in plates coated with 10 μg/mL fibronectin (Sigma-Aldrich, Steinheim, Germany).

Primary Cell Culture

Cells were cultured at 37°C in a humidified 5% CO_2 environment. Culture medium was refreshed every 2–3 days. Cells were passed using trypsin-EDTA (Sigma-Aldrich) at 70%–80% (HUAFs) or 90%–100% (HUVECs) confluency. HUAFs were used up to passage five, and HUVECs were used up to passage three. Stock solutions of isolated HUAFs and HUVECs up to passage two were stored at −180°C in DMEM GlutaMAX containing 20% FBS and 10% DMSO (Sigma-Aldrich).

In Vitro Ischemia Model

For *in vitro* ischemia experiments, HUAFs were seeded in separate 12-well plates at 70,000 cells per well and subsequently cultured in either: control conditions for 48 h (normal culture medium and ~20% oxygen), 48-h ischemic conditions (starvation medium and hypoxia of 1% oxygen), or 24-h ischemic conditions (initial 24 h in normal culture medium and ~20% oxygen followed by 24 h in starvation medium and hypoxia of 1% oxygen). Starvation medium consisted of DMEM GlutaMAX (Invitrogen) with 0.1% heat-inactivated FBS (PAA) and 100 U penicillin and 100 μg streptomycin per milliliter (Lonza). For consistency with the 24-h ischemic-condition group, medium of the 48-h control condition and 48-h ischemic condition groups was also refreshed after 24 h. At the end of the experiment, cells were washed with PBS and harvested with TRIzol Reagent (Invitrogen).

RNA Isolation and cDNA Synthesis

Total RNA was isolated with TRIzol (Invitrogen) according to the manufacturer's instructions. RNA concentration and purity were examined by NanoDrop (NanoDrop Technologies, Wilmington, DE, USA). For pri-miRNA experiments, DNase treatment was performed using RQ1 RNase-Free DNase (Promega, Madison, WI, USA) according to the manufacturer's instructions. Total cDNA was prepared using the High Capacity cDNA Reverse Transcription Kit (Applied Biosystems, Foster City, CA, USA) according to the manufacturer's protocol.

Specific Quantification of WT- and ISO-miR-411 by 5′DB-PCR

The expression of WT-miR-411 and ISO-miR-411 was quantified using a self-designed TaqMan qPCR assay specific enough to distinguish the 1-nt difference at the 5′ end of the miRNAs. The assay

was designed and performed based on the previously described 5′DB-PCR method.[56,57] An overview of primer, probe, and adaptor sequences is provided in Table S2.

In brief, 50 ng total RNA was combined with 5 pmol synthetic 5′ adapters (synthesized by Integrated DNA Technologies; IDT), which are specific for either WT-miR-411 or ISO-miR-411. After heating the samples to 90°C for 3 min, the samples were buffered with Tris-HCl and $MgCl_2$ (Invitrogen) (final concentration, 5 mM and 10 mM, respectively [pH 8.0]). The 5′ adapters were then annealed to the WT-miR-411 or ISO-miR-411 within the sample (20 min at 37°C) and subsequently ligated to each other at 37°C for 30 min using T4 RNA Ligase 2 (Rnl2; New England Biolabs, Ipswich, MA, USA), followed by overnight incubation at 4°C. After reheating the samples to 90°C for 2 min, reverse transcription of the ligated RNA was performed using the High Capacity cDNA Reverse Transcription Kit (Applied Biosystems) and a miR-411-specific RT primer (1 μM). The expression of WT-miR-411 and ISO-miR-411 within cDNA samples was quantified by qPCR using WT-miR-411- or ISO-miR-411-specific PrimeTime LNA probes combined with a primer set specific for the ligated RNA product. The specificity of the assay was confirmed using synthetic sequences (Figure S1). qPCRs were performed on the ViiA7 Real-Time PCR System (Applied Biosystems) using TaqMan Universal PCR Master Mix (Applied Biosystems). miR-411 expression was normalized against noncoding household RNA *U6*, also quantified by a TaqMan assay (Applied Biosystems). In all graphs, the expression of WT-miR-411 and ISO-miR-411 is presented as fold change, relative to the expression of WT-miR-411 in the control condition.

WT-pre-miR-411 and ISO-pre-miR-411 were quantified using the same 5′DB-PCR method but instead using pre-miR-411-specific primers.

Quantification of mRNA Expression

The expression of mRNAs within cDNA samples was quantified by qPCR using Quantitect SYBR Green (QIAGEN) on the ViiA7 Real-Time PCR System (Applied Biosystems). mRNA expression was measured with intron-spanning primers and normalized against *RPLP0* mRNA expression, a household gene that remains stable under ischemic conditions.[28] All primer sequences are provided in Table S3.

siRNA-Mediated Knockdown of ADAR1 and ADAR2

Knockdown of ADAR1 and ADAR2 in HUAFs was performed as previously described.[29] Briefly, HUAFs were seeded in 12-well plates, grown to 70% confluence, and then transfected using Lipofectamine RNAiMAX (Invitrogen) according to the manufacturer's protocol, with a final concentration of 27.5 nM siRNA. siRNA sequences used were originally reported and validated by Stellos et al.[28] and can be found in Table S6. After 48 h, cells were washed 3 times with PBS, total RNA was isolated, and cDNA was synthesized as described earlier. Expression of *ADAR1*, *ADAR2*, and *RPLP0* was quantified to determine knockdown efficiency. Subsequent microRNA expression analyses were performed as described earlier.

HLI Model

All animal experiments were approved by the committee on animal welfare of the Leiden University Medical Center (Leiden, the Netherlands, approval reference number 09163).

Adult male C57BL/6 mice, 8 to 12 weeks old (Charles River, Wilmington, MA, USA) were housed in groups of 3 to 5 animals, with free access to tap water and regular chow. The assignment of the mice to the experimental groups was conducted randomly.

Induction of HLI was performed as described previously.[29] In brief, mice were anesthetized by intraperitoneal injection of midazolam (5 mg/kg, Roche Diagnostics, Almere, the Netherlands), medetomidine (0.5 mg/kg, Orion, Espoo, Finland), and fentanyl (0.05 mg/kg, Janssen Pharmaceuticals, Beerse, Belgium). Unilateral HLI was induced by electrocoagulation of the left femoral artery proximal to the superficial epigastric arteries. After surgery, anesthesia was antagonized with flumazenil (0.5 mg/kg, Fresenius Kabi, Bad Homburg vor der Höhe, Germany), atipamezole (2.5 mg/kg, Orion), and buprenorphine (0.1 mg/kg, MSD Animal Health, Boxmeer, the Netherlands). Mice were sacrificed by cervical dislocation, and the adductor and gastrocnemius muscles were excised en bloc and snap-frozen on dry ice before (T0) and at 1 and 3 days after induction of HLI (T1 and T3, respectively). Muscle tissues were crushed with pestle and mortar while using liquid nitrogen to preserve sample integrity. Tissue homogenates were stored at −80°C. Total RNA was isolated from tissue powder by standard TRIzol-chloroform extraction as described earlier.

Collection of Human LLV Samples

Human LLV samples were collected at the Leiden University Medical Center.

Surplus LLV tissue from patients with CAD was collected during coronary bypass surgery. These samples were anonymized, and no data were recorded that could potentially trace back to an individual's identity. Collection, storage, and processing of the samples were performed in compliance with the Medical Treatment Contracts Act (WGBO, 1995) and the Code of Conduct for Health Research using Body Material (Good Practice Code, Dutch Federation of Biomedical Scientific Societies, 2002) and the Dutch Personal Data Protection Act (WBP, 2001).

Furthermore, LLVs from 8 patients with end-stage PAD were obtained directly after lower limb amputation. Inclusion criteria for the biobank were a minimum age of 18 years and lower limb amputation, excluding ankle, foot, or toe amputations. The exclusion criteria were suspected or confirmed malignancy and the inability to give informed consent. Sample collection was approved by the Medical Ethics Committee of the Leiden University Medical Center (protocol no. P12.265), and written informed consent was obtained from these participants.

All LLV samples were snap-frozen and stored at −80°C. Frozen LLV tissues were crushed in liquid nitrogen, and total RNA was isolated

from tissue powder by standard TRIzol-chloroform extraction as described earlier.

In Silico Target Prediction and Pathway Enrichment Analysis

Putative targetomes of WT-miR-411 and ISO-miR-411 were determined using three distinct target prediction algorithms to reduce the number of false positives: Targetscan (http://www.targetscan.org),[33] miRanda (http://www.microRNA.org),[58] and Diana-MR-microT (http://diana.imis.athena-innovation.gr).[59] Targetscan v6.2 and miRanda (2010 release) predictions were obtained through the miRmut2go webtool (http://compbio.uthsc.edu/miR2GO),[60] whereas Diana-MR-microT predictions were obtained using its website. No restrictions were applied for target prediction. Genes were only considered to be a particular microRNA's putative target gene if each of the 3 target prediction algorithms identified them as a target.

For each targetome, the set of target genes of a particular microRNA, overrepresented pathways were identified using PANTHER pathway enrichment analysis (v11; http://www.pantherdb.org)[34] as described previously.[61]

Dual Luciferase Reporter Gene Assays

Constructs

3′ UTR sequences containing one or more WT-miR-411 or ISO-miR-411 binding sites from endogenous target genes were amplified from HUAF cDNA using primers with a short extension containing cleavage sites for XhoI (5′ end) and NotI (3′ end) (Table S3). For *ANGPT1*, the endogenous binding sequence was purchased from IDT (Coralville, IA, USA) instead (Table S4).

Amplicons and synthetic sequences were cloned in the PsiCHECK-2 vector (Promega) at the 3′ end of the coding region of the Renilla luciferase reporter gene. The sequence of each construct was confirmed.

Sequences of the primers used are available in Table S3.

Luciferase Assays

HeLa cells were cultured at 37°C under 5% CO_2 using DMEM (GIBCO) with high glucose and stable L-glutamine supplemented with 10% fetal calf serum and 100 U penicillin and 100 μg streptomycin per milliliter (Lonza). For experiments, HeLa cells were grown to 75%–80% confluence in white 96-well plates. Lipofectamine 3000 (Invitrogen) in Opti-MEM (GIBCO) was used, according to the manufacturer's instructions, to transfect each well with 30 ng PsiCHECK2-vector containing endogenous miRNA binding sequences or the original empty vector. Cells were co-transfected with 2 pmol miRcury LNA miRNA Mimic for a WT-miR-411, ISO-miR-411, or negative-control miRNA (QIAGEN). Firefly and Renilla luciferase were measured in cell lysates using the Dual-Luciferase Reporter Assay System (Promega) according to the manufacturer's protocol on a Cytation 5 plate reader (BioTek Instruments, Winooski, VT, USA). Firefly luciferase activity was used as an internal control for cellular density and transfection efficiency. The luminescence ratios were corrected for differences in baseline vector luminescence observed in the vehicle-treated group and expressed as percentage of scrambled control luminescence.

Displayed luciferase data represent the normalized averages from three independent experiments.

Endogenous Transcript Regulation by WT-miR-411 or ISO-miR-411

Endogenous transcript regulation was examined by overexpression of WT-miR-411 or ISO-miR-411 in HUAFs. HUAFs were seeded in 12-well plates at 70,000 cells per well and grown for 12 h in culture medium after which the medium was replaced with starvation medium to synchronize cell cycle. After another 12h, Lipofectamine RNAiMAX (Invitrogen) in Opti-MEM (GIBCO) was used according to the manufacturer's instructions to transfect each well with 0.1 pg miRcury LNA miRNA Mimic for a WT-miR-411, ISO-miR-411, or negative control miRNA (QIAGEN). After 12 h, the transfection medium was replaced with new starvation medium. After 14 h (26 h total after transfection), cells were washed twice with PBS and harvested with TRIzol Reagent, after which RNA was isolated, total cDNA was prepared, and target mRNA expression was measured by qPCR as described earlier. Target mRNA expression was normalized against *RPLP0*. The intron spanning primers used can be found in Table S3. Displayed endogenous target regulation represents the normalized averages from three independent experiments.

Regulation of TGFB2 and ANGPT1 by WT-miR-411 or ISO-miR-411

Endogenous protein regulation was also examined by overexpression of WT-miR-411 or ISO-miR-411 in HUAFs through transfection. This time, 50,000 cells were seeded per well in 12-well plates to grow for 12 h in culture medium followed by synchronization by switching to starvation medium for 6 h. HUAFs were then transfected with 0.1 pg miRcury LNA miRNA Mimic for a WT-miR-411, ISO-miR-411, or negative-control miRNA (QIAGEN) using Opti-MEM (GIBCO) and Lipofectamine RNAiMAX (Invitrogen) according to the manufacturer's instructions. 48 h after transfection, conditioned medium was collected, and cells were washed twice with PBS and harvested with TRIzol Reagent (Invitrogen).

No TGFB2 could be detected in the HUAF conditioned medium using the Human TGF-beta 2 Quantikine ELISA Kit (DB250, R&D Systems, Minneapolis, MN, USA) according to the manufacturer's instructions. Therefore, protein was isolated from cell lysates with TRIzol (Invitrogen), according to the manufacturer's instructions. Total protein concentration was quantified by the Pierce BCA Protein Assay Kit (Thermo Fisher Scientific), after which protein concentration was normalized to 1 μg/μL in Laemmli buffer (Bio-Rad Laboratories, Hercules, CA, USA) containing 10% β-mercaptoethanol (Sigma-Aldrich).

Samples were heated to 95°C for 5 min and cooled before loading 1 μg of protein per lane in a 4%–15% Mini-PROTEAN TGM Precast

Protein Gel (Bio-Rad Laboratories). Protein separation was performed in the Vertical Electrophoresis Cell system using premixed Tris/glycine/SDS running buffer (both Bio-Rad Laboratories). Proteins were transferred onto a nitrocellulose membrane (GE Healthcare Life Sciences, Eindhoven, the Netherlands) by a wet transfer using premixed Tris/glycine transfer buffer (Bio-Rad Laboratories). The membrane was blocked at room temperature in 5% non-fat dried milk in TBS-T (150 mM NaCl, 50 mM Tris, and 0.05% Tween-20; Sigma-Aldrich) and subsequently incubated overnight at 4°C with antibodies for TGFB2 (ab36495, Abcam, Cambridge, UK) or stable household protein vinculin (hVIN-1; Novus Biologicals, Centennial, CO, USA) diluted to 1:500 in 5% non-fat dried milk in TBS-T. After multiple washes with TBS-T, the membrane was incubated at room temperature with anti-mouse peroxidase-conjugated secondary antibody (31432, Thermo Fisher Scientific) diluted to 1:10.000 in 5% non-fat dried milk in TBS-T. Proteins of interest were revealed using SuperSignal West Pico PLUS Chemiluminescent Substrate (ThermoFisher Scientific) and imaged using the ChemiDoc Touch Imaging System (Bio-Rad Laboratories). TGFB2 expression was quantified relative to stable household protein vinculin using ImageJ.

Levels of secreted ANGPT1 in HUAF conditioned medium were quantified using the Human Angiopoietin-1 Quantikine ELISA Kit (DANG10, R&D Systems, Minneapolis, MN, USA) according to the manufacturer's instructions.

Displayed endogenous protein regulation represents the normalized averages from three independent experiments.

Scratch-Wound Healing Assays

Effects of WT-miR-411 or ISO-miR-411 overexpression on scratch-wound healing of HUAFs were examined. HUAFs were seeded and transfected as described earlier. Transfection medium was removed after 12 h. Next, a p200 pipette tip was used to introduce a scratch wound across the diameter of each well. Subsequently, the cells were washed with sterile PBS, and medium was replaced with new serum starvation medium. Three locations along the scratch wound were marked per well. The scratch wounds at these sites were imaged at times 0 h and 14 h after scratch-wound introduction using live phase-contrast microscopy (Axiovert 40 C, Carl Zeiss Microscopy, Oberkochen, Germany). After the 14-h time point, cells were washed 3 times in PBS and then lysed and harvested in TRIzol for RNA isolation as described earlier. miRNA overexpression efficiency was validated by measuring miRNA expression as described earlier. For each imaged location, the area of the scratch wound at 0 h was superimposed on the 14-h scratch-wound area image. Scratch-wound healing was then determined per well as the newly covered scratch-wound area after 14 h using the wound-healing tool macro for ImageJ. Displayed scratch-wound healing represents the averages from three independent experiments.

Statistical Analysis

All results are expressed as mean ± SEM. Since all variables measured were continuous parameters, pairwise comparisons were tested using t tests. p values less than or equal to 0.05 were considered statistically significant.

SUPPLEMENTAL INFORMATION

Supplemental Information can be found online at https://doi.org/10.1016/j.ymthe.2019.10.002.

AUTHOR CONTRIBUTIONS

Conceptualization, A.Y.N. and P.H.A.Q.; Methodology, R.V.C.T.v.d.K. and A.Y.N.; Investigation, R.V.C.T.v.d.K. and T.W.; Writing – Original Draft, R.V.C.T.v.d.K.; Writing – Review & Editing, R.V.C.T.v.d.K., T.W., P.H.A.Q., and A.Y.N.; Funding Acquisition, A.Y.N.; Supervision, P.H.A.Q. and A.Y.N.

CONFLICTS OF INTEREST

The authors declare no competing interests.

ACKNOWLEDGMENTS

We thank M.R. de Vries for obtaining the HLI samples and E.A.C. Goossens, K.H. Simons, and the vascular and thoracic surgeons of the LUMC who collected the patient material. This study was supported by a grant from the Dutch Heart Foundation (Dr. E. Dekker, Senior Postdoc; 2014T102), the LUMC Johanna Zaaijer Fund (2017), and the Austrian Science Fund FWF (Lise Meitner Grant; M 2578-B30).

REFERENCES

1. Bartel, D.P. (2004). MicroRNAs: genomics, biogenesis, mechanism, and function. Cell *116*, 281–297.
2. Zhao, Y., Ransom, J.F., Li, A., Vedantham, V., von Drehle, M., Muth, A.N., Tsuchihashi, T., McManus, M.T., Schwartz, R.J., and Srivastava, D. (2007). Dysregulation of cardiogenesis, cardiac conduction, and cell cycle in mice lacking miRNA-1-2. Cell *129*, 303–317.
3. Weber, C. (2013). MicroRNAs: from basic mechanisms to clinical application in cardiovascular medicine. Arterioscler. Thromb. Vasc. Biol. *33*, 168–169.
4. Welten, S.M., Goossens, E.A., Quax, P.H., and Nossent, A.Y. (2016). The multifactorial nature of microRNAs in vascular remodelling. Cardiovasc. Res. *110*, 6–22.
5. Friedman, R.C., Farh, K.K., Burge, C.B., and Bartel, D.P. (2009). Most mammalian mRNAs are conserved targets of microRNAs. Genome Res. *19*, 92–105.
6. Brennecke, J., Stark, A., Russell, R.B., and Cohen, S.M. (2005). Principles of microRNA-target recognition. PLoS Biol. *3*, e85.
7. Lewis, B.P., Shih, I.H., Jones-Rhoades, M.W., Bartel, D.P., and Burge, C.B. (2003). Prediction of mammalian microRNA targets. Cell *115*, 787–798.
8. Han, J., Lee, Y., Yeom, K.H., Nam, J.W., Heo, I., Rhee, J.K., Sohn, S.Y., Cho, Y., Zhang, B.T., and Kim, V.N. (2006). Molecular basis for the recognition of primary microRNAs by the Drosha-DGCR8 complex. Cell *125*, 887–901.
9. Neilsen, C.T., Goodall, G.J., and Bracken, C.P. (2012). IsomiRs–the overlooked repertoire in the dynamic microRNAome. Trends Genet. *28*, 544–549.
10. Lee, Y., Ahn, C., Han, J., Choi, H., Kim, J., Yim, J., Lee, J., Provost, P., Rådmark, O., Kim, S., and Kim, V.N. (2003). The nuclear RNase III Drosha initiates microRNA processing. Nature *425*, 415–419.
11. Ha, M., and Kim, V.N. (2014). Regulation of microRNA biogenesis. Nat. Rev. Mol. Cell Biol. *15*, 509–524.
12. Kobayashi, H., and Tomari, Y. (2016). RISC assembly: coordination between small RNAs and Argonaute proteins. Biochim. Biophys. Acta *1859*, 71–81.
13. Kozomara, A., Birgaoanu, M., and Griffiths-Jones, S. (2019). miRBase: from microRNA sequences to function. Nucleic Acids Res. *47* (D1), D155–D162.

14. Landgraf, P., Rusu, M., Sheridan, R., Sewer, A., Iovino, N., Aravin, A., Pfeffer, S., Rice, A., Kamphorst, A.O., Landthaler, M., et al. (2007). A mammalian microRNA expression atlas based on small RNA library sequencing. Cell *129*, 1401–1414.

15. Kuchenbauer, F., Morin, R.D., Argiropoulos, B., Petriv, O.I., Griffith, M., Heuser, M., Yung, E., Piper, J., Delaney, A., Prabhu, A.L., et al. (2008). In-depth characterization of the microRNA transcriptome in a leukemia progression model. Genome Res. *18*, 1787–1797.

16. Starega-Roslan, J., Krol, J., Koscianska, E., Kozlowski, P., Szlachcic, W.J., Sobczak, K., and Krzyzosiak, W.J. (2011). Structural basis of microRNA length variety. Nucleic Acids Res. *39*, 257–268.

17. Wu, H., Ye, C., Ramirez, D., and Manjunath, N. (2009). Alternative processing of primary microRNA transcripts by Drosha generates 5′ end variation of mature microRNA. PLoS ONE *4*, e7566.

18. Cloonan, N., Wani, S., Xu, Q., Gu, J., Lea, K., Heater, S., Barbacioru, C., Steptoe, A.L., Martin, H.C., Nourbakhsh, E., et al. (2011). MicroRNAs and their isomiRs function cooperatively to target common biological pathways. Genome Biol. *12*, R126.

19. Llorens, F., Bañez-Coronel, M., Pantano, L., del Río, J.A., Ferrer, I., Estivill, X., and Martí, E. (2013). A highly expressed miR-101 isomiR is a functional silencing small RNA. BMC Genomics *14*, 104.

20. Loher, P., Londin, E.R., and Rigoutsos, I. (2014). IsomiR expression profiles in human lymphoblastoid cell lines exhibit population and gender dependencies. Oncotarget *5*, 8790–8802.

21. Telonis, A.G., Loher, P., Jing, Y., Londin, E., and Rigoutsos, I. (2015). Beyond the one-locus-one-miRNA paradigm: microRNA isoforms enable deeper insights into breast cancer heterogeneity. Nucleic Acids Res. *43*, 9158–9175.

22. Telonis, A.G., Magee, R., Loher, P., Chervoneva, I., Londin, E., and Rigoutsos, I. (2017). Knowledge about the presence or absence of miRNA isoforms (isomiRs) can successfully discriminate amongst 32 TCGA cancer types. Nucleic Acids Res. *45*, 2973–2985.

23. Small, E.M., and Olson, E.N. (2011). Pervasive roles of microRNAs in cardiovascular biology. Nature *469*, 336–342.

24. Welten, S.M., Bastiaansen, A.J., de Jong, R.C., de Vries, M.R., Peters, E.A., Boonstra, M.C., Sheikh, S.P., La Monica, N., Kandimalla, E.R., Quax, P.H., and Nossent, A.Y. (2014). Inhibition of 14q32 MicroRNAs miR-329, miR-487b, miR-494, and miR-495 increases neovascularization and blood flow recovery after ischemia. Circ. Res. *115*, 696–708.

25. Muiwo, P., Pandey, P., Ahmad, H.M., Ramachandran, S.S., and Bhattacharya, A. (2018). IsomiR processing during differentiation of myelogenous leukemic cell line K562 by phorbol ester PMA. Gene *641*, 172–179.

26. Bandara, V., Michael, M.Z., and Gleadle, J.M. (2014). Hypoxia represses microRNA biogenesis proteins in breast cancer cells. BMC Cancer *14*, 533.

27. Bandara, K.V., Michael, M.Z., and Gleadle, J.M. (2017). MicroRNA biogenesis in hypoxia. MicroRNA *6*, 80–96.

28. Stellos, K., Gatsiou, A., Stamatelopoulos, K., Perisic Matic, L., John, D., Lunella, F.F., Jaé, N., Rossbach, O., Amrhein, C., Sigala, F., et al. (2016). Adenosine-to-inosine RNA editing controls cathepsin S expression in atherosclerosis by enabling HuR-mediated post-transcriptional regulation. Nat. Med. *22*, 1140–1150.

29. van der Kwast, R.V.C.T., van Ingen, E., Parma, L., Peters, H.A.B., Quax, P.H.A., and Nossent, A.Y. (2018). Adenosine-to-inosine editing of microRNA-487b alters target gene selection after ischemia and promotes neovascularization. Circ. Res. *122*, 444–456.

30. Nishikura, K., Sakurai, M., Ariyoshi, K., and Ota, H. (2013). Antagonistic and stimulative roles of ADAR1 in RNA silencing. RNA Biol. *10*, 1240–1247.

31. Nishikura, K. (2016). A-to-I editing of coding and non-coding RNAs by ADARs. Nat. Rev. Mol. Cell Biol. *17*, 83–96.

32. Hellingman, A.A., Bastiaansen, A.J., de Vries, M.R., Seghers, L., Lijkwan, M.A., Lowik, C.W., Hamming, J.F., and Quax, P.H. (2010). Variations in surgical procedures for hind limb ischaemia mouse models result in differences in collateral formation. Eur. J. Vasc. Endovasc. Surg. *40*, 796–803.

33. Agarwal, V., Bell, G.W., Nam, J.W., and Bartel, D.P. (2015). Predicting effective microRNA target sites in mammalian mRNAs. eLife *4*, e05005.

34. Mi, H., Huang, X., Muruganujan, A., Tang, H., Mills, C., Kang, D., and Thomas, P.D. (2017). PANTHER version 11: expanded annotation data from Gene Ontology and Reactome pathways, and data analysis tool enhancements. Nucleic Acids Res. *45* (D1), D183–D189.

35. Bofill-De Ros, X., Yang, A., and Gu, S. (2019). IsomiRs: expanding the miRNA repression toolbox beyond the seed. Biochim. Biophys. Acta. Gene Regul. Mech. Published online April 4, 2019. https://doi.org/10.1016/j.bbagrm.2019.03.005.

36. Fukunaga, R., Han, B.W., Hung, J.H., Xu, J., Weng, Z., and Zamore, P.D. (2012). Dicer partner proteins tune the length of mature miRNAs in flies and mammals. Cell *151*, 533–546.

37. Ma, H., Wu, Y., Choi, J.G., and Wu, H. (2013). Lower and upper stem-single-stranded RNA junctions together determine the Drosha cleavage site. Proc. Natl. Acad. Sci. USA *110*, 20687–20692.

38. Gebert, L.F.R., and MacRae, I.J. (2019). Regulation of microRNA function in animals. Nat. Rev. Mol. Cell Biol. *20*, 21–37.

39. Guo, Y., Liu, J., Elfenbein, S.J., Ma, Y., Zhong, M., Qiu, C., Ding, Y., and Lu, J. (2015). Characterization of the mammalian miRNA turnover landscape. Nucleic Acids Res. *43*, 2326–2341.

40. Kim, Y., Yeo, J., Lee, J.H., Cho, J., Seo, D., Kim, J.S., and Kim, V.N. (2014). Deletion of human tarbp2 reveals cellular microRNA targets and cell-cycle function of TRBP. Cell Rep. *9*, 1061–1074.

41. Ota, H., Sakurai, M., Gupta, R., Valente, L., Wulff, B.E., Ariyoshi, K., Iizasa, H., Davuluri, R.V., and Nishikura, K. (2013). ADAR1 forms a complex with Dicer to promote microRNA processing and RNA-induced gene silencing. Cell *153*, 575–589.

42. Heale, B.S.E., Keegan, L.P., McGurk, L., Michlewski, G., Brindle, J., Stanton, C.M., Caceres, J.F., and O'Connell, M.A. (2009). Editing independent effects of ADARs on the miRNA/siRNA pathways. EMBO J. *28*, 3145–3156.

43. Cho, C.J., Myung, S.J., and Chang, S. (2017). ADAR1 and microRNA; a hidden cross-talk in cancer. Int. J. Mol. Sci. *18*, E799.

44. Michlewski, G., and Cáceres, J.F. (2019). Post-transcriptional control of miRNA biogenesis. RNA *25*, 1–16.

45. Downie Ruiz Velasco, A., Welten, S.M.J., Goossens, E.A.C., Quax, P.H.A., Rappsilber, J., Michlewski, G., and Nossent, A.Y. (2019). Posttranscriptional regulation of 14q32 microRNAs by the CIRBP and HADHB during vascular regeneration after ischemia. Mol. Ther. Nucleic Acids *14*, 329–338.

46. Welten, S.M.J., de Vries, M.R., Peters, E.A.B., Agrawal, S., Quax, P.H.A., and Nossent, A.Y. (2017). Inhibition of Mef2a enhances neovascularization via post-transcriptional regulation of 14q32 microRNAs miR-329 and miR-494. Mol. Ther. Nucleic Acids *7*, 61–70.

47. Treiber, T., Treiber, N., Plessmann, U., Harlander, S., Daiß, J.L., Eichner, N., Lehmann, G., Schall, K., Urlaub, H., and Meister, G. (2017). A compendium of RNA-binding proteins that regulate microRNA biogenesis. Mol. Cell *66*, 270–284.e13.

48. Hofer, E., and Schweighofer, B. (2007). Signal transduction induced in endothelial cells by growth factor receptors involved in angiogenesis. Thromb. Haemost. *97*, 355–363.

49. Li, C., Guo, B., Bernabeu, C., and Kumar, S. (2001). Angiogenesis in breast cancer: the role of transforming growth factor beta and CD105. Microsc. Res. Tech. *52*, 437–449.

50. Chen, J., Kasper, M., Heck, T., Nakagawa, K., Humpert, P.M., Bai, L., Wu, G., Zhang, Y., Luther, T., Andrassy, M., et al. (2005). Tissue factor as a link between wounding and tissue repair. Diabetes *54*, 2143–2154.

51. Xu, Z., Xu, H., Ploplis, V.A., and Castellino, F.J. (2010). Factor VII deficiency impairs cutaneous wound healing in mice. Mol. Med. *16*, 167–176.

52. Koh, G.Y. (2013). Orchestral actions of angiopoietin-1 in vascular regeneration. Trends Mol. Med. *19*, 31–39.

53. Novotny, N.M., Lahm, T., Markel, T.A., Crisostomo, P.R., Wang, M., Wang, Y., Tan, J., and Meldrum, D.R. (2009). Angiopoietin-1 in the treatment of ischemia and sepsis. Shock *31*, 335–341.

54. Cho, S., Jang, I., Jun, Y., Yoon, S., Ko, M., Kwon, Y., Choi, I., Chang, H., Ryu, D., Lee, B., et al. (2013). MiRGator v3.0: a microRNA portal for deep sequencing, expression profiling and mRNA targeting. Nucleic Acids Res. *41*, D252–D257.

55. Zhang, Y., Zang, Q., Xu, B., Zheng, W., Ban, R., Zhang, H., Yang, Y., Hao, Q., Iqbal, F., Li, A., and Shi, Q. (2016). IsomiR Bank: a research resource for tracking IsomiRs. Bioinformatics *32*, 2069–2071.

56. Shigematsu, M., Honda, S., and Kirino, Y. (2018). Dumbbell-PCR for discriminative quantification of a small RNA variant. Methods Mol. Biol. *1680*, 65–73.

57. Honda, S., and Kirino, Y. (2015). Dumbbell-PCR: a method to quantify specific small RNA variants with a single nucleotide resolution at terminal sequences. Nucleic Acids Res. *43*, e77.

58. Betel, D., Koppal, A., Agius, P., Sander, C., and Leslie, C. (2010). Comprehensive modeling of microRNA targets predicts functional non-conserved and non-canonical sites. Genome Biol. *11*, R90.

59. Paraskevopoulou, M.D., Georgakilas, G., Kostoulas, N., Vlachos, I.S., Vergoulis, T., Reczko, M., Filippidis, C., Dalamagas, T., and Hatzigeorgiou, A.G. (2013). DIANA-microT web server v5.0: service integration into miRNA functional analysis workflows. Nucleic Acids Res. *41*, W169–W173.

60. Bhattacharya, A., and Cui, Y. (2015). miR2GO: comparative functional analysis for microRNAs. Bioinformatics *31*, 2403–2405.

61. Mi, H., Muruganujan, A., Casagrande, J.T., and Thomas, P.D. (2013). Large-scale gene function analysis with the PANTHER classification system. Nat. Protoc. *8*, 1551–1566.